Letter

Polarization Dependence of Surface-Enhanced Raman Scattering in Gold Nanoparticle#Nanowire Systems

Hong Wei, Feng Hao, Yingzhou Huang, Wenzhong Wang, Peter Nordlander, and Hongxing Xu

More About This Article

Additional resources and features associated with this article are available within the HTML version:

- Supporting Information
- Links to the 2 articles that cite this article, as of the time of this article download
- Access to high resolution figures
- Links to articles and content related to this article
- Copyright permission to reproduce figures and/or text from this article

View the Full Text HTML

Polarization Dependence of Surface-Enhanced Raman Scattering in Gold Nanoparticle−Nanowire Systems

Hong Wei,[†] Feng Hao,[‡] Yingzhou Huang,[†] Wenzhong Wang,[†,§] Peter Nordlander,*,[‡] and Hongxing Xu*,[†,||]

Laboratory of Soft Matter Physics, Beijing National Laboratory for Condensed Matter Physics and Institute of Physics, Chinese Academy of Sciences, Box 603-146, 100190, Beijing, China, Laboratory for Nanophotonics, Department of Physics and Astronomy, Rice University, Houston, Texas 77005-1892, School of Science, Central University for Nationalities, Beijing 100081, China, and Division of Solid State Physics/The Nanometer Structure Consortium, Lund University, Box 118, S-221 00, Lund, Sweden

ABSTRACT

We study the polarization dependence of surface-enhanced Raman scattering (SERS) in coupled gold nanoparticle−nanowire systems. The coupling between the continuous nanowire plasmons and the localized nanoparticle plasmons results in significant field enhancements and SERS enhancements comparable to those found in nanoparticle dimer junctions. The SERS intensity is maximal when the incident light is polarized across the particle and the wire, and the enhancement is remarkably insensitive to the detailed geometrical structures of the nanoparticles.

Metal nanostructures are of considerable current interest because of their highly tunable optical properties.[1–7] The excitation of surface plasmons can generate greatly enhanced electromagnetic fields, which provide the dominant contributions to the enhancement factors in surface-enhanced Raman scattering (SERS).[8–10] SERS has been widely explored as an analytical tool for chemical and biological sensing since its discovery about thirty years ago.[9,11,12] Much recent research has focused on the development of an understanding of how the structural properties of metallic nanostructures can be optimized to provide the largest possible electromagnetic field enhancements. These studies have shown that the largest enhancement factors typically occur in junctions between coupled nanoparticles when illuminated by light polarized across the junction between the particles.[13–16] The intense electric fields induced in such junctions when illuminated by light of a wavelength in resonance with the coupled nanoparticle plasmon are believed to be the "hot spots" for Raman scattering which dominates the observed SERS signal in more complex nanoparticle aggregates. The polarization dependence of SERS "hot spots" has been investigated for many different metal nanostructures, such as nanoparticle aggregates,[17–19] aligned nanowire rafts,[20] aligned nanorod arrays,[21] coupled nanowires,[22] and single Ag nanowires.[23]

Nanoparticles and finite nanowires are two important elementary nanostructures which have attracted great interest as SERS substrates because of the relative simplicity with which they can be fabricated.[13,14,24–27] A uniform long metallic wire cannot couple to light because of the mismatch of the photon and wire plasmon dispersion relations. In a recent study, it was shown that a metallic nanoparticle adjacent to a metallic wire can serve as an efficient nanoantenna providing a means for coupling light into and out from propagating wire plasmons.[28] The mechanisms underlying this antenna action is the electromagnetic coupling between the plasmons in the individual nanoparticle and nanowire. A theoretical analysis has predicted that the magnitude of this coupling should be insensitive to the detailed shape of the nanoparticle but exhibit a strong polarization dependence and be accompanied by large local and polarization dependent electric field enhancements in the nanoparticle−wire junctions.[29] Such field enhancements can strongly enhance the Raman scattering if probe molecules are located in the junctions between the two nanostructures.

In this work, we have studied the polarization dependence of SERS in the coupled gold nanoparticle−nanowire system

* Corresponding authors. E-mail: nordland@rice.edu (P.N.) and hxxu@aphy.iphy.ac.cn (H.X.).
† Chinese Academy of Sciences.
‡ Rice University.
§ Central University for Nationalities.
|| Lund University.
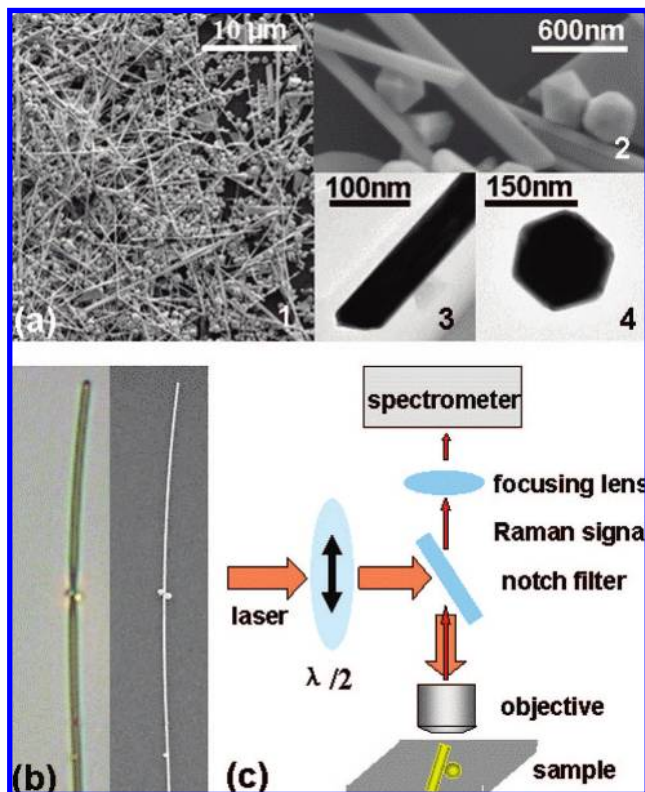
Figure 1. (a) SEM images (1 and 2) and TEM images (3 and 4) of the gold wire and particle samples. (b) optical microscopy (left) and SEM (right) images of a nanowire–particle aggregate. The part of the nanowire in (b) is about 40 μm long. (c) Sketch of the experimental setup.

for nanoparticles of a variety of shapes. We find that the SERS spectra are strongly enhanced when the incident light is polarized across the junction between the particle and the wire and remarkably insensitive to the detailed geometrical structure of the nanoparticle. The measured Raman enhancements are in good agreement with theoretical predictions.

Gold nanoparticles and nanowires were prepared using chemical fabrication. For the synthesis of Au wires and particles, 444 mg poly(vinyl pyrrolidone) (PVP, MW = 30 000) was dissolved into 40 mL solution of ethylene glycol (EG) with the help of continuous magnetic stirring. Then 0.01 mL NaBH$_4$ solution (0.2 M) was introduced. After 2 min, 0.3 mL of a HAuCl$_4$ solution (0.5 M) was added. The mixture was kept at 50 °C for 6 h in an ultrasonic bath first, then transferred into a Teflon vessel and sealed in a stainless-steel bomb. The container was kept at 160 °C for 12 h in a furnace and finally cooled to room temperature. The product was washed via centrifugation three times in ethanol to remove EG and PVP. The precipitates were collected and dissolved in ethanol for future use. Scanning electron microscopy (SEM) images show that both nanowires and nanoparticles with different shapes and sizes are included in the product. It is surprising that the gold nanowires can be tens of micrometers long. In Figure 1a, typical SEM images and transmission electron microscopy (TEM) images of the samples are shown.

Malachite green isothiocyanate (MGITC) was employed as probe molecules. A dilute mixture of Au particles and
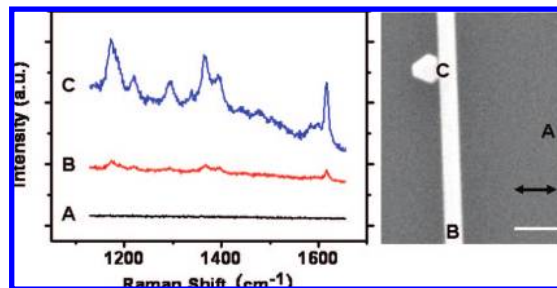
Figure 2. Raman spectra of MGITC from different positions of the sample. The scale bar is 400 nm. The arrow in the SEM image shows the incident polarization. The laser power on sample is 380 μW and the exposure time is 2 s.

wires were incubated with 65 μM MGITC ethanol solution of the same volume for 1 h. Then 10 μL of the incubated mixture was spin-coated on clean Si substrates with a size of about 1.5 cm × 1.5 cm. The density of molecules on both the metal surface and the substrate surface is estimated to be about a monolayer. Colloidal gold nanoparticles were easily observed to deposit near the gold wires by optical microscope, where the light scattering is different from the bare trunk of the nanowire, which was later confirmed with SEM images. A TEM grid was fixed on the sample with tape as marks for the identification of the positions investigated.[18] With the help of the grid, the detailed geometry of identified individual nanoparticle–wire aggregates can be imaged with SEM. An example of a wire–particle aggregate is shown in Figure 1b. The optical microscopy and SEM images agree well. The SERS spectra were measured with a Renishaw inVia microRaman spectroscopy system. The samples were excited by a 632.8 nm He–Ne laser through a 50 × (NA = 0.75) objective resulting in a spot size of around 2 μm in diameter. The Raman signal was collected with the same objective in a backscattering geometry. The polarization of the incident laser was changed using a half-wave plate. The different responses of the Raman system for different incident polarizations are corrected by the normalization factor of the Raman scattering of HOPG at 1580 cm^{-1}. A schematic illustration of the experimental setup is shown in Figure 1c.

Typical SERS spectra of MGITC are shown in Figure 2a. Depending on the different probe positions, shown in Figure 2b, the SERS spectra of MGITC are enhanced differently. No SERS spectra can be observed from Si substrate without Ag nanostructures, although MGITC is strongly resonant at the incident wavelength of 633 nm. For a probe position on the trunk of the Ag nanowire, however, weak SERS spectra can be observed. The polarization dependence of this SERS spectra (data not shown) is similar to what was observed recently for SERS of brilliant crystal blue on individual Ag nanowires.[23] Surprisingly, when a particle was located near a wire with the incident polarization across the junction between nanoparticle and wire, the Raman intensity is significantly enhanced. This is due to the coupling between the particle and the wire plasmons and will be discussed below. The result in Figure 2 clearly shows that the nanoparticle–wire junction provides a "hot-spot" for SERS.
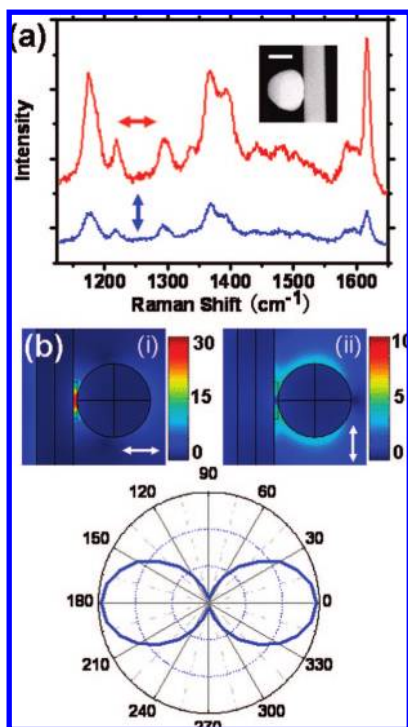
Figure 3. (a) SERS spectra of MGITC at two different polarizations for the wire−particle shown in the inset. The scale bar in the inset is 200 nm. The laser power is 70 μW, and the exposure time is 10 s. (b) Calculated electric field for a gold sphere of radius 50 at 5 nm from a wire of radius 25 nm for perpendicular (i) and parallel (ii) polarization to the wire. The polar graph shows the calculated SERS enhancement in the junction between nanoparticle and nanowire as a function of polarization angle.

Figure 3 shows typical SERS spectra of MGITC from a nanoparticle−nanowire aggregate under different polarizations. The intensity of the spectra changes as the polarization of the incident light is varied. When the laser is polarized parallel to the wire, the Raman intensity is weak. When the laser is polarized perpendicularly to the wire, the Raman intensity increases. The SEM image of the wire−particle sample is shown in the inset. Finite element analysis simulations using commercial software (COMSOL Multiphysics) were used to study the spatial distribution of the electric fields. The simulations are performed by modeling the nanoparticle and wire using periodic boundary conditions with a unit cell of 500 nm. The size of this unit cell is sufficiently large that the effects of nanoparticle−nanoparticle interactions can be neglected. The separation between the nanoparticle and the wire is assumed to be 5 nm. The dielectric properties of Au are modeled using the experimentally measured Johnson and Christy's data.[30]

The results from the simulations show that the electric field enhancements are considerably larger for polarization perpendicular to the wire than for polarization parallel to the wire. For SERS, it is generally agreed that the Raman intensity increases by a factor E^4.[8–10] The first two powers of the enhancement is due to the local electromagnetic (EM) field enhancement associated with the incident light, while the second two powers of the enhancement factor is the Raman emission (RE) enhancement caused by the antenna

effect of metal nanostructures. These two contributions to the SERS enhancement are not necessarily the same. For a junction between a nanoparticle and a nanowire, the local electrical field $|E_{loc}(\omega_L,\theta)| = |E_{max}(\omega_L)| \cos(\theta)$, where $E_{max}(\omega_L)$ is the maximum of the local electric field $E_{loc}(\omega_L,\theta)$ for the optimal polarization, ω_L is the laser frequency, and θ is the polarization angle of the incident light with respect to a surface normal of the wire pointing to the nanoparticle. Hence, the local EM enhancement $|E_{loc}(\omega_L,\theta)/E_0(\omega_L)|^2 = |E_{max}(\omega_L)/E_0(\omega_L)|^2 \cos^2(\theta)$ will have a simple $\cos^2(\theta)$ polarization dependence. However, the direction of the induced electric field in the junction is always in the direction across the junction ($\theta = 0$) and independent of the incident polarization. This means that the induced Raman dipole at the Raman frequency ω_R and its Raman emission behavior will be polarization independent leading to a RE factor proportional to $|E_{max}(\omega_R)/E_0(\omega_R)|^2$, where $E_{max}(\omega_R)$ is the maximum of the local electric field $E_{loc}(\omega_R,\theta)$ for the optimal polarization, and $E_0(\omega_R)$ is the corresponding incident field at the Raman frequency ω_R. Thus, the total SERS enhancement factor is proportional to

$$G_{junction} = \left|\frac{E_{max}(\omega_L)}{E_0(\omega_L)}\right|^2 \left|\frac{E_{max}(\omega_R)}{E_0(\omega_R)}\right|^2 \cos^2(\theta) \approx \left|\frac{E_{max}}{E_0}\right|^4 \cos^2(\theta) \ (1)$$

where the $\cos^2(\theta)$ factor originates from the EM contribution, and the last approximation results from the assumption that the electric field enhancements at ω_L and ω_R are approximately the same. This argument can be generalized to SERS from arbitrary metallic structures. Since the direction of the induced electric field is always normal to the metal surface and independent of the incident polarization, the RE enhancement factor will be polarization independent. Thus, for any polarization dependent measurement, the normal fourth power local SERS enhancement should be modified to

$$G = \left|\frac{E_{loc}(\omega_L, \theta)}{E_0(\omega_L)}\right|^2 \left|\frac{E_{max}(\omega_R)}{E_0(\omega_R)}\right|^2 \qquad (2)$$

where E_{loc} is the actual polarization dependent local electric field, and $E_{max}(\omega_R)$ is the maximum local field at the Raman frequency that can be obtained at that point for the optimal polarization. If the Raman frequency ω_R is very close to the laser frequency ω_L, $E_{max}(\omega_R)$ can be assumed to be the same as the maximum of the local electric field $E_{loc}(\omega_L,\theta)$ for the optimal polarization. Otherwise, the local electric field $E_{loc}(\omega_R,\theta)$ at the Raman frequency and the corresponding $E_{max}(\omega_R)$ can be different. Figure 3b shows the simulation results of the local electric field enhancement, and the polar plot shows the calculated SERS enhancement in the junction between nanoparticle and nanowire for different polarizations using eq 1). The polarization dependence of the calculated electric field enhancements are in qualitative agreement with the Raman intensities in Figure 3a. The weaker but still appreciable SERS enhancement observed in Figure 3a for polarization parallel to the nanowire is most likely caused by SERS from molecules adsorbed outside the junction and will be further discussed below.

In Figure 4, the measured SERS intensity at the Raman peak of 1616 cm^{-1} of MGITC as a function of polarization angle θ (defined in the inset) are shown for three different shapes of nanoparticles. For the rod−wire (a) and triangular
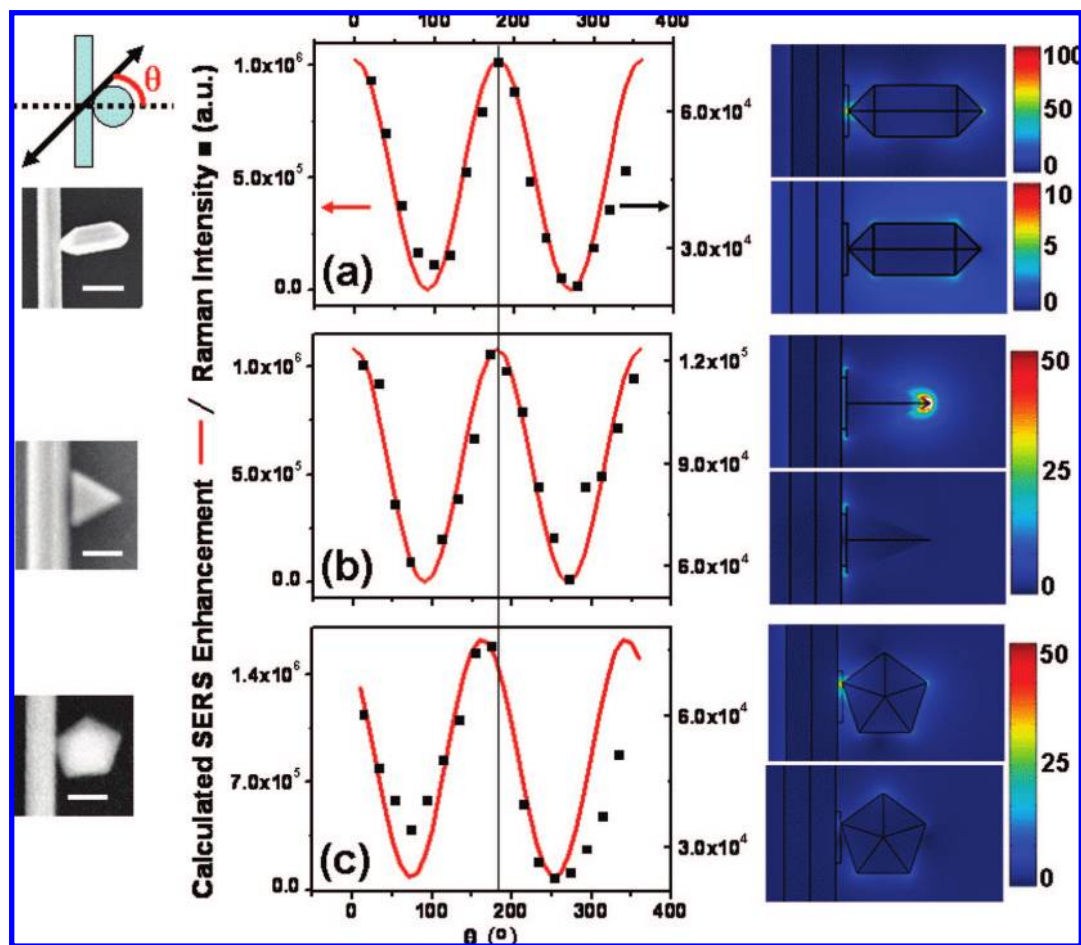
Figure 4. Measured (squares) and calculated (lines) SERS intensity as a function of polarization angle θ defined in the inset for different shape particles adjacent to a wire. The measured intensity is the 1616 cm^{-1} peak (integrated from 1610 cm^{-1} to 1620 cm^{-1}) in the SERS spectra of MGITC. The laser power is 70 μW, and the exposure time is 10 s. The SEM images of the wire−particle system investigated are shown on the left, and the electric field distributions from theoretical calculations are shown on the right for perpendicular polarization (upper plot) and parallel polarization (lower plot). The scale bar in the SEM images is 1 μm in (a) and 200 nm in (b) and (c).

particle−wire (b), the Raman intensity is maximal for $\theta = 0$ (180°), while for the star−wire systems (c), the maximum Raman intensity bias is slightly about −10° from $\theta = 0$ (180°), which may be caused by the unsymmetrical configuration of pentagon star−wire system. To theoretically estimate the SERS enhancement, we use COMSOL and average eq 2 in a thin layer of thickness 2 nm over the surface of the nanoparticle at the wavelength of the incident light 633 nm. Numerical tests show the choice of the integration volume will only affect the absolute intensity of the resulting Raman enhancement but has little impact for its polarization dependence.

The calculated SERS enhancements in Figure 4 are in very good agreement with the experimental measurements. The calculated intensities are found to be proportional to $\cos^2(\theta)$ similar to several previous studies for nanoparticle aggregates.[19,22,31] The theoretical calculations show that, for perpendicular polarization, most of the calculated Raman intensity arises from the nanoparticle/wire junction. For parallel polarization, the dominant part of the calculated Raman intensity originates from the outer surfaces of the nanoparticle with the junction surface only contributing a few percent to the total Raman signal. It should be noted

that the experimental data for parallel polarization ($\theta = 90°$) are slightly larger than the theoretical predictions. The calculated Raman intensity for $\theta = 90°$ for a nanoparticle near a uniform individual wire was found to give a negligible Raman signal and we believe that the experimentally observed larger signal for $\theta = 90°$ is due to Raman scattering from molecules adsorbed near defects of the wire. The calculated SERS enhancement and the polarization dependence are insensitive to the shapes of the particles, which indicate the plasmon coupling between particle and wire plays a more important role for the SERS enhancement than the detailed shape of the nanoparticle. It should also be noted that the coupling between local particle plasmon and continuous wire plasmon can give very large local SERS enhancements. For the separation between particle and wire of 5 nm, the averaged SERS enhancement is in the order of 10^6 for the different shapes of the particles, and the maximum local SERS enhancement for perpendicular polarization is of the order of 10^{10} which is similar to the maximum local enhancements calculated in nanoparticle dimer junctions.[15]

The optical properties of the coupled metallic spherical particle and wire system have been studied analytically in the electrostatic limit using the plasmon hybridization
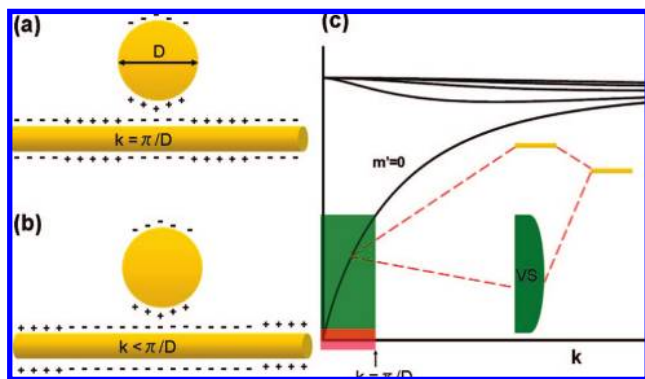
Figure 5. Schematic illustration of the coupling of a nanoparticle to the symmetric ($m' = 0$) wire plasmon continuum. (a,b) The nanoparticle can couple efficiently to symmetric wire plasmons of half-wavelengths larger than the diameter D. (c) Plasmon hybridization in the metallic nanoparticle wire system. The red area illustrates the wave vectors of the wire plasmon that couple efficiently to the nanoparticle and the green area shows their energies. The VS continuum can couple efficiently to light because of the admixture of nanoparticle plasmons with dipolar moments.

method.[29] For an infinite wire, the plasmons are continuous states characterized by wave vector along the axis and their azimuthal symmetry. When a finite nanoparticle is placed in the proximity of the wire, the discrete plasmon states of the particle will hybridize with the wire plasmon continuum through electromagnetic interactions. The nature of the interaction is schematically illustrated in Figure 5.

The interaction results in a bonding plasmonic VS and an antibonding localized state.[29] The VS is primarily composed of long wavelength wire plasmons and is optically active because of the finite admixture of dipolar nanoparticle plasmons. The nanoparticle serves as a nanoantenna that when polarized by the incident light couples efficiently to wire plasmons of half-wavelengths larger than the diameter of the nanoparticle. The wave vector distribution of wire plasmons that make up the VS does not depend on the detailed shape of the nanoparticle but only on its lateral dimension along the wire. The energies of the wire plasmons that participate in the VS are determined by the wire plasmon dispersion relations which are dependent on the radius of the wire. The composition and spectral properties of the plasmonic VS are thus determined by the nanoparticle and wire diameters rather than by the detailed geometric structure of the nanoparticle. The plasmon hybridization study shows that the intensity and spectral features of the virtual state depend strongly on the polarization of the incident light. For polarization perpendicular to the wire, the polarization charges on the particle are closer to the wire compared with the case with parallel polarization, which leads to a stronger coupling, higher intensity of the virtual state and larger field enhancement in the junction between the particle and the wire.

In order to determine the spectral properties of the virtual states, we have calculated the extinction spectrum for nanospheres of radii 25 and 50 nm at 5 nm from the wire using COMSOL and the finite-difference time-domain (FDTD) method. For both systems, the VS appears in the range of $800-1000$ nm. This suggests that larger Raman signals could be achieved if a laser source at this wavelength regime is used instead of the present 632.8 nm He−Ne laser.

In conclusion, we have investigated the polarization dependence of SERS in coupled gold nanoparticle−nanowire systems. We have shown that the SERS enhancement in the particle−wire junctions results from the electromagnetic coupling between the plasmons in the individual nanoparticle and nanowire which leads to large field enhancement. The SERS enhancement is strongest when the incident light is polarized across the junction and is insensitive to the detailed geometrical structure of the particle. The experimental results agree well with theoretical calculations.

Supporting Information Available: Raman mapping of a gold nanowire−nanoparticle system and more examples showing polarization dependence. This material is available free of charge via the Internet at http://pubs.acs.org.

References

(1) Wang, H.; Brandl, D. W.; Le, F.; Nordlander, P.; Halas, N. J. *Nano Lett.* **2006**, *6*, 827–832.
(2) Nehl, C. L.; Liao, H. W.; Hafner, J. H. *Nano Lett.* **2006**, *6*, 683–688.
(3) Aizpurua, J.; Hanarp, P.; Sutherland, D. S.; Kall, M.; Bryant, G. W.; de Abajo, F. J. G. *Phys. Rev. Lett.* **2003**, *90*, 057401.
(4) Bukasov, R.; Shumaker-Parry, J. S. *Nano Lett.* **2007**, *7*, 1113–1118.
(5) Prikulis, J.; Hanarp, P.; Olofsson, L.; Sutherland, D.; Kall, M. *Nano Lett.* **2004**, *4*, 1003–1007.
(6) Lassiter, J. B.; Aizpurua, J.; Hernandez, L. I.; Brandl, D. W.; Romero, I.; Lal, S.; Hafner, J. H.; Nordlander, P.; Halas, N. J. *Nano Lett.* **2008**, *8*, 1212–1218.
(7) Bryant, G. W.; de Abajo, F. J. G.; Aizpurua, J. *Nano Lett.* **2008**, *8*, 631–636.
(8) Moskovits, M. *Rev. Mod. Phys.* **1985**, *57*, 783–826.
(9) Kneipp, K.; Kneipp, H.; Itzkan, I.; Dasari, R. R.; Feld, M. S. *Chem. Rev.* **1999**, *99*, 2957–2975.
(10) Schatz, G. C.; Young, M. A.; Van Duyne, R. P. *Top. Appl. Phys.* **2006**, *103*, 19–45.
(11) Kneipp, K.; Kneipp, H.; Itzkan, I.; Dasari, R. R.; Feld, M. S. *J. Phys.: Condens. Matter* **2002**, *14*, R597–R624.
(12) Willets, K. A.; Van Duyne, R. P. *Annu. Rev. Phys. Chem.* **2007**, *58*, 267–297.
(13) Xu, H. X.; Bjerneld, E. J.; Kall, M.; Borjesson, L. *Phys. Rev. Lett.* **1999**, *83*, 4357–4360.
(14) Michaels, A. M.; Jiang, J.; Brus, L. E. *J. Phys. Chem. B* **2000**, *104*, 11965–11971.
(15) Xu, H. X.; Aizpurua, J.; Kall, M.; Apell, P. *Phys. Rev. E* **2000**, *62*, 4318–4324.
(16) Sawai, Y.; Takimoto, B.; Nabika, H.; Ajito, K.; Murakoshi, K. *J. Am. Chem. Soc.* **2007**, *129*, 1658–1662.
(17) Bosnick, K. A.; Jiang, J.; Brus, L. E. *J. Phys. Chem. B* **2002**, *106*, 8096–8099.
(18) Xu, H. X.; Kall, M. *Chemphyschem* **2003**, *4*, 1001–1005.
(19) Etchegoin, P. G.; Galloway, C.; Le Ru, E. C. *Phys. Chem. Chem. Phys.* **2006**, *8*, 2624–2628.
(20) Jeong, D. H.; Zhang, Y. X.; Moskovits, M. *J. Phys. Chem. B* **2004**, *108*, 12724–12728.
(21) Zhao, Y. P.; Chaney, S. B.; Shanmukh, S.; Dluhy, R. A. *J. Phys. Chem. B* **2006**, *110*, 3153–3157.
(22) Tao, A. R.; Yang, P. D. *J. Phys. Chem. B* **2005**, *109*, 15687–15690.

(23) Mohanty, P.; Yoon, I.; Kang, T.; Seo, K.; Varadwaj, K. S. K.; Choi, W.; Park, Q. H.; Ahn, J. P.; Suh, Y. D.; Ihee, H.; Kim, B. *J. Am. Chem. Soc.* **2007**, *129*, 9576–9577.

(24) Braun, G.; Lee, S. J.; Dante, M.; Nguyen, T. Q.; Moskovits, M.; Reich, N. *J. Am. Chem. Soc.* **2007**, *129*, 6378–6379.

(25) Talley, C. E.; Jackson, J. B.; Oubre, C.; Grady, N. K.; Hollars, C. W.; Lane, S. M.; Huser, T. R.; Nordlander, P.; Halas, N. J. *Nano Lett.* **2005**, *5*, 1569–1574.

(26) Lee, S. J.; Morrill, A. R.; Moskovits, M. *J. Am. Chem. Soc.* **2006**, *128*, 2200–2201.

(27) Tao, A.; Kim, F.; Hess, C.; Goldberger, J.; He, R. R.; Sun, Y. G.; Xia, Y. N.; Yang, P. D. *Nano Lett.* **2003**, *3*, 1229–1233.

(28) Knight, M. W.; Grady, N. K.; Bardhan, R.; Hao, F.; Nordlander, P.; Halas, N. J. *Nano Lett* **2007**, *7*, 2346–2350.

(29) Hao, F.; Nordlander, P. *Appl. Phys. Lett.* **2006**, *89*, 103101.

(30) Johnson, P. B.; Christy, R. W. *Phys. Rev. B* **1972**, *6*, 4370–4379.

(31) Jiang, J.; Bosnick, K.; Maillard, M.; Brus, L. *J. Phys. Chem. B* **2003**, *107*, 9964–9972.